Comput Mech (2007) 40:461–472
DOI 10.1007/s00466-006-0121-2

ORIGINAL PAPER

An adaptive fast multipole boundary element method for three-dimensional acoustic wave problems based on the Burton–Miller formulation

L. Shen · Y. J. Liu

Received: 18 November 2005 / Accepted: 25 August 2006 / Published online: 7 October 2006

Abstract The high solution costs and non-uniqueness difficulties in the boundary element method (BEM) based on the conventional boundary integral equation (CBIE) formulation are two main weaknesses in the BEM for solving exterior acoustic wave problems. To tackle these two weaknesses, an adaptive fast multipole boundary element method (FMBEM) based on the Burton–Miller formulation for 3-D acoustics is presented in this paper. In this adaptive FMBEM, the Burton–Miller formulation using a linear combination of the CBIE and hypersingular BIE (HBIE) is applied to overcome the non-uniqueness difficulties. The iterative solver generalized minimal residual (GMRES) and fast multipole method (FMM) are adopted to improve the overall computational efficiency. This adaptive FMBEM for acoustics is an extension of the adaptive FMBEM for 3-D potential problems developed by the authors recently. Several examples on large-scale acoustic radiation and scattering problems are presented in this paper which show that the developed adaptive FMBEM can be several times faster than the non-adaptive FMBEM while maintaining the accuracies of the BEM.

Keywords Fast multipole method · Boundary element method · Helmholtz equation · Burton–Miller formulation

L. Shen · Y. J. Liu (✉)
Computer-Aided Engineering Research Laboratory,
Department of Mechanical Engineering,
University of Cincinnati, Cincinnati, OH 45221-0072, USA
e-mail: Yijun.Liu@uc.edu

1 Introduction

The boundary element method (BEM) (See, e.g., [1,2]) is a numerical approach for solving field problems based on the boundary integral equation (BIE) formulations. The BEM has been used to solve exterior acoustic problems for many years (See, e.g., [3–7]), because of its boundary only discretization and automatically satisfaction of the radiation condition at infinity. The BEM, however, has some drawbacks. The most troublesome one is that the BEM leads to systems of equations with dense, non-symmetrical and sometimes ill-conditioned coefficient matrices. Solving the BEM system of equations needs $O(N^3)$ operations with N being the number of unknowns, when direct solvers, such as the Gauss elimination method [8], are used. As a result, the BEM is prohibitively expensive when it is used to solve large-scale engineering problems.

Improving the overall solution efficiency has been the main task in the implementation of the BEM. Much work has been devoted to finding efficient solvers for BEM systems of equations. Iterative solvers, such as the generalized minimum residue (GMRES) method [9] and the conjugate gradient squared (CGS) method [10] have been proved to be beneficial. Iterative solvers perform matrix-vector multiplication in each iteration, which needs $O(N^2)$ operations in the conventional way. Consequently, the total number of operation counts for the BEM with iterative solver is reduced from $O(N^3)$ to $O(N^2)$.

To further improve the efficiency of the BEM with iterative solvers, various techniques have been proposed to accelerate the matrix–vector multiplication. These techniques include the wavelet basis [11], the H-matrices [12], the fast Fourier transform [13] and the fast

multipole method [14,15]. Among all the methods mentioned above, the fast multipole method (FMM) seems to be the most widely accepted method in fast BEM implementations.

The FMM was first proposed by Greengard and Rokhlin [14,15] to accelerate the evaluation of interactions of large ensembles of particles governed by Laplace equation. The key idea behind the FMM is a multipole expansion of the kernel in which the connection between the collocation point and the source point is separated. Many research works have been published since then to improve and extend the applicability of the FMM [16–20]. Employing the FMM for the matrix–vector multiplications in iterative solvers, the computing cost can be reduced from $O(N^2)$ to $O(N)$. The FMM was later extended to Helmholtz equation (See, e.g., [21–39]). Rokhlin [23] and Lu and Chew [25] proposed diagonal form of the translation matrices for high frequency Helmholtz. Wagner and Chew [26] used ray propagation approach to further accelerate the FMM for high frequency range. Greengard et al. [33] suggested diagonal translation for low frequency range. Gumerov and Duraiswami [36] extended recurrence relations reported in Chew's paper [40] to develop a general recursive method for obtaining the translation matrices. For a comprehensive review on the fast multipole method, a state-of-the-art review paper was given by Nishimura [41].

With the FMM and iterative solver, we are able to construct fast multipole boundary element method (FMBEM) that is based on the conventional BIE. However, there is a defect; the conventional BIE fails to yield unique solutions for exterior acoustic problems at the eigen-frequencies associated with the corresponding interior problems. For mathematical explanation of the eigen-frequencies associated with the CBIE, please see [5] and a comprehensive review paper by Chen and Hong [42].

To deal with the non-uniqueness difficulties, several methods have been proposed in the last several decades. Combined Helmholtz integral equation formulation (CHIEF) proposed by Schenck [4] can successfully remove the non-uniqueness by adding some additional Helmholtz integral relations in the interior domain, which leads to an over-determined system of equations. The CHIEF method suffers from the difficulty that there are no methods so far to analytically determine the number of interior points and their locations. As the wave number increases, the number of eigen-frequencies is more likely to increase, and more interior points are required to maintain accuracy, leading to the loss of efficiency.

An alternative way to overcome the non-uniqueness difficulties is the Burton–Miller formulation [5]. It uses a linear combination of the conventional BIE (CBIE) and the normal derivative of the conventional BIE (HBIE) to circumvent this problem. It has been proved [5] that the combined BIE (CHBIE) yields unique solutions in all frequency range for exterior acoustic problems. The downside of this approach is that the number of integrations doubles. Even worse, it requires the evaluation of the hypersingular integral with a kernel of double normal derivatives of the Green's function. Several methods have been suggested to evaluate the hypersingular integral, including the direct evaluation in the Hadamard-finite-part sense [43], regularization with Taylor series expansions [44,45] or Fourier–Legendre series [46], transformation into integrals with kernel of tangential derivatives or double surface integrals [5] and indirect evaluations [6]. Although hypersingular integral evaluation is no longer a big challenge and iterative solvers can accelerate the Burton–Miller based BEM as well, a total of four integral evaluations for each pair of elements is still an expansive task with the conventional BEM approach, which further restricts the use of the Burton–Miller based BEM.

Applying the FMM in the iterative solver for the Burton–Miller based BEM will improve this situation. The advantages of combining the Burton–Miller BIE with the FMBEM are twofold. First, the non-uniqueness difficulty is resolved by using Burton–Miller formulation. Second, the overall solution efficiency is improved by adopting the FMM within the iterative solver. In this study, an adaptive algorithm extended from the one reported in [47] is developed that can further improve the efficiency of the Burton–Miller based FMBEM.

The paper is organized as follows: the basic FMBEM formulation is reviewed in Sect. 2. The new adaptive FMBEM algorithm is presented in Sect. 3. In Sect. 4, the applicability of the adaptive Burton–Miller based FMBEM is investigated with several radiation and scattering problems. Section 5 concludes the paper with further discussions.

2 Formulations

2.1 Conventional BEM formulation

The propagation of time-harmonic acoustic waves in a homogeneous isotropic acoustic medium E (which can be either finite or infinite) is described by the Helmholtz equation:

$$\nabla^2\varphi(\mathbf{x}) + k^2\varphi(\mathbf{x}) = 0 \quad \forall\, \mathbf{x} \in E, \tag{1}$$

where φ is the velocity potential, $k = \omega/c$ the wavenumber, ω the angular frequency, and c the wave speed in the acoustic medium E.

The boundary conditions for Helmholtz equation take the following form:

$$\begin{aligned} &\varphi(\mathbf{x}) = \bar{\varphi}(\mathbf{x}), \quad \forall\, \mathbf{x} \in S_1; \\ &q(\mathbf{x}) = \bar{q}(\mathbf{x}), \quad \forall\, \mathbf{x} \in S_2; \end{aligned} \tag{2}$$

where $q(\mathbf{x})$ is the normal derivative of φ at point $\mathbf{x}$, $S = S_1 \cup S_2$ is the boundary of E, and the barred quantities indicate given values on the boundary.

The integral representation of the solution to Helmholtz equation is:

$$\varphi(\mathbf{x}) = \int_S \left[G(\mathbf{x},\mathbf{y}) q(\mathbf{y}) - \frac{\partial G(\mathbf{x},\mathbf{y})}{\partial n(\mathbf{y})} \varphi(\mathbf{y}) \right] \mathrm{d}S(\mathbf{y}) + \varphi^I(\mathbf{x}) \quad \forall\, \mathbf{x} \in E, \tag{3}$$

where $\mathbf{x}$ is the collocation point, $\mathbf{y}$ the source point. The free-space Green's function G for 3-D problems is given by:

$$G(\mathbf{x},\mathbf{y}) = \frac{\mathrm{e}^{ikr}}{4\pi r}, \quad \text{with } r = |\mathbf{x} - \mathbf{y}|, \tag{4}$$

where $\mathrm{i} = \sqrt{-1}$ and $n(\mathbf{y})$ the outward normal at $\mathbf{y}$. The incident wave $\varphi^I(\mathbf{x})$ in Eq. (3) will not present for radiation problems.

Letting point $\mathbf{x}$ approach the boundary leads to the following conventional boundary integral equation (CBIE):

$$C(\mathbf{x})\varphi(\mathbf{x}) = \int_S \left[G(\mathbf{x},\mathbf{y}) q(\mathbf{y}) - \frac{\partial G(\mathbf{x},\mathbf{y})}{\partial n(\mathbf{y})} \varphi(\mathbf{y}) \right] \mathrm{d}S(\mathbf{y}) + \varphi^I(\mathbf{x}) \quad \forall\, \mathbf{x} \in S, \tag{5}$$

where the constant $C(\mathbf{x}) = 1/2$, if S is smooth around $\mathbf{x}$.

Taking the derivative of integral representation (3) with respect to the normal at the collocation point $\mathbf{x}$ ($n(\mathbf{x})$) and letting $\mathbf{x}$ approach S give the following hypersingular boundary integral equation (HBIE):

$$C(\mathrm{x})q(\mathrm{x}) = \int_S \left[\frac{\partial G(\mathbf{x},\mathbf{y})}{\partial n(\mathbf{x})} q(\mathbf{y}) - \frac{\partial^2 G(\mathbf{x},\mathbf{y})}{\partial n(\mathbf{y}) \partial n(\mathbf{x})} \varphi(\mathbf{y}) \right] \mathrm{d}S(\mathbf{y}) + q^I(\mathbf{x}) \quad \forall\, \mathbf{x} \in S, \tag{6}$$

where $C(\mathbf{x}) = 1/2$ if S is smooth around $\mathbf{x}$. Both CBIE Eq. (5) and HBIE Eq. (6) describe the behavior of the acoustic velocity potential on the surface of the body. For an exterior problem, they have a different set of fictitious frequencies at which a unique solution for the exterior problem cannot be obtained. However, Eqs. (5) and (6) will always have only one solution in common. Given this fact, the following linear combination of Eqs. (5) and (6) (CHBIE) should yield a unique solution for all frequencies [5]:

$$\begin{aligned} &\left[\int_S \frac{\partial G(\mathbf{x},\mathbf{y})}{\partial n(\mathbf{y})} \varphi(\mathbf{y}) \mathrm{d}S(\mathbf{y}) + C(\mathbf{x})\varphi(\mathbf{x}) - \varphi^I(\mathbf{x}) \right] \\ &\quad + \alpha \int_S \frac{\partial^2 G(\mathbf{x},\mathbf{y})}{\partial n(\mathbf{y}) \partial n(\mathbf{x})} \varphi(\mathbf{y}) \mathrm{d}S(\mathbf{y}) = \int_S G(\mathbf{x},\mathbf{y}) q(\mathbf{y}) \mathrm{d}S(\mathbf{y}) \\ &\quad + \alpha \left[\int_S \frac{\partial G(\mathbf{x},\mathbf{y})}{\partial n(\mathbf{x})} q(\mathbf{y}) \mathrm{d}S(\mathbf{y}) - C(\mathbf{x}) q(\mathbf{x}) + q^I(\mathbf{x}) \right] \\ &\quad \forall\, \mathbf{x} \in S, \end{aligned} \tag{7}$$

where α is a coupling constant that can be chosen as i/k [48]. This CHBIE formulation is referred to as the Burton–Miller formulation.

The discretized form of the Burton–Miller formulation can be obtained by discretizing the boundary S using N (e.g., constant) surface elements:

$$\sum_{j=1}^{N} f_{ij}\varphi_j = \sum_{j=1}^{N} g_{ij} q_j + \widehat{b}_i \quad \text{for node } i = 1, 2, \ldots, N, \tag{8}$$

where $\widehat{b}_i$ is from the incident wave for scattering problems, and

$$\begin{aligned} f_{ij}\varphi_j &= \int_{\Delta S_j} \frac{\partial G(\mathrm{x},\mathrm{y})}{\partial n(\mathrm{y})} \varphi_j \mathrm{d}S(\mathrm{y}) + \frac{1}{2}\delta_{ij}\varphi_j \\ &\quad + \alpha \int_{\Delta S_j} \frac{\partial^2 G(\mathrm{x},\mathrm{y})}{\partial n(\mathrm{y}) \partial n(\mathrm{x})} \varphi_j \mathrm{d}S(\mathrm{y}), \\ g_{ij} q_j &= \int_{\Delta S_j} G(\mathrm{x},\mathrm{y}) q_j \mathrm{d}S(\mathrm{y}) \\ &\quad + \alpha \left[\int_{\Delta S_j} \frac{\partial G(\mathrm{x},\mathrm{y})}{\partial n(\mathrm{x})} q_j \mathrm{d}S(\mathrm{y}) - \frac{1}{2}\delta_{ij} q_j \right], \end{aligned} \tag{9}$$

with δ_{ij} being the Kronecker δ-symbol and ΔS_j representing element j. Equation (9) implies that for each pair of elements (i, j), there are a total of four integrals that need to be evaluated.

Rearranging each term in Eq. (8), that is, moving the unknown terms to the left-hand side and known terms to the right-hand side, gives the following system of equations:

$$\begin{bmatrix} a_{11} & a_{12} & \cdots & a_{1N} \\ a_{21} & a_{22} & \cdots & a_{2N} \\ \vdots & \vdots & \ddots & \vdots \\ a_{N1} & a_{N2} & \cdots & a_{NN} \end{bmatrix} \begin{Bmatrix} \lambda_1 \\ \lambda_2 \\ \vdots \\ \lambda_N \end{Bmatrix} = \begin{Bmatrix} b_1 \\ b_2 \\ \vdots \\ b_N \end{Bmatrix}, \quad \text{or} \quad \mathbf{A}\lambda = \mathbf{b}, \tag{10}$$

where **A** is the system matrix, λ the unknown vector, and **b** the known vector.

The singular and hypersingular integrations in Eq. (9) are evaluated using the singularity subtraction approach (See, e.g., [44,45]). In this approach, the singularity in the singular or hypersingular integral is regularized first using a one-term or two-term subtraction, respectively. Then the added back term (with static Green's function) is evaluated analytically, which is possible with the use of constant elements. The analytical integration has the benefit of accuracy and efficiency and is well suited for integration with the FMBEM.

2.2 The fast multipole method

The fast multipole method is employed to solve the Burton–Miller BIE, or CHBIE Eq. (7), for which iterative solver GMRES will be used and the system of equations (10) will not be formed explicitly. Several expansions and translations are needed in the FMM and most of these formulas for Helmholtz equation are well documented in [27,49]. They are listed in this section for completeness in order to discuss the developed adaptive algorithm in the following section.

The free-space Green's function in Eq. (4) can be expressed as a multipole expansion around an expansion point $\mathbf{y}_c$ near $\mathbf{y}$ (Fig. 1):

$$G(\mathbf{x},\mathbf{y}) = \frac{ik}{4\pi}\sum_{n=0}^{\infty}(2n+1)\sum_{m=-n}^{n}\bar{I}_n^m(k,\mathbf{y},\mathbf{y}_c)O_n^m(k,\mathbf{x},\mathbf{y}_c), \quad \text{for } |\mathbf{y}-\mathbf{y}_c| < |\mathbf{x}-\mathbf{y}_c|, \tag{11}$$

where the inner function I_n^m is in the form:

$$I_n^m(k,\mathbf{y},\mathbf{y}_c) = j_n(k|\mathbf{y}-\mathbf{y}_c|)Y_n^m\left(\frac{\mathbf{y}-\mathbf{y}_c}{|\mathbf{y}-\mathbf{y}_c|}\right), \tag{12}$$

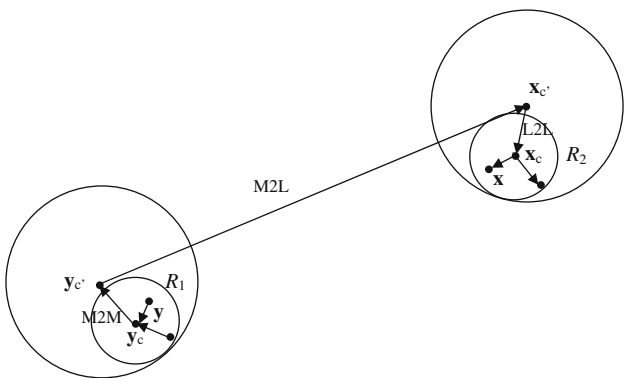

Fig. 1 M2M, M2L and L2L translations

with $\bar{I}_n^m$ being the complex conjugate of I_n^m, and the outer function O_n^m is defined by:

$$O_n^m(k,\mathbf{x},\mathbf{y}_c) = h_n^{(1)}(k|\mathbf{x}-\mathbf{y}_c|)Y_n^m\left(\frac{\mathbf{x}-\mathbf{y}_c}{|\mathbf{x}-\mathbf{y}_c|}\right). \tag{13}$$

In the above Eqs. (11–13), Y_n^m are spherical harmonics; j_n the nth order spherical Bessel function of the first kind; h_n the nth order spherical Hankel function of the first kind. For integrals on element j which are far away from the collocation point $\mathbf{x}$ ($|\mathbf{y}-\mathbf{y}_c| < |\mathbf{x}-\mathbf{y}_c|$), the integrations in Eq. (9) can then be written as the multipole expansions around $\mathbf{y}_c$ as follows:

$$\left.\begin{aligned}&\int_{\Delta S_j} G(\mathbf{x}_i,\mathbf{y})q_j\mathrm{d}S(\mathbf{y})\\ &\int_{\Delta S_j}\frac{\partial G(\mathbf{x}_i,\mathbf{y})}{\partial n(\mathbf{y})}\varphi_j\mathrm{d}S(\mathbf{y})\end{aligned}\right\} = \frac{ik}{4\pi}\sum_{n=0}^{\infty}(2n+1)\sum_{m=-n}^{n}M_{n,j}^m(k,\mathbf{y}_c)O_n^m(k,\mathbf{x}_i,\mathbf{y}_c),$$
$$\left.\begin{aligned}&\int_{\Delta S_j}\frac{\partial G(\mathbf{x}_i,\mathbf{y})}{\partial n(\mathbf{x}_i)}q_j\mathrm{d}S(\mathbf{y})\\ &\int_{\Delta S_j}\frac{\partial^2 G(\mathbf{x}_i,\mathbf{y})}{\partial n(\mathbf{y})\partial n(\mathbf{x}_i)}\varphi_j\mathrm{d}S(\mathbf{y})\end{aligned}\right\} = \frac{ik}{4\pi}\sum_{n=0}^{\infty}(2n+1)\sum_{m=-n}^{n}M_{n,j}^m(k,\mathbf{y}_c)\frac{O_n^m(k,\mathbf{x}_i,\mathbf{y}_c)}{\partial n(\mathbf{x}_i)}, \tag{14}$$

where $M_{n,j}^m$ are called multipole moments defined by:

$$M_{n,j}^m(k,\mathbf{y}_c) = \begin{cases}\displaystyle\int_{\Delta S_j}\bar{I}_n^m(k,\mathbf{y},\mathbf{y}_c)q_j\mathrm{d}S(\mathbf{y}), & \text{for } g_{ij}q_j;\\ \displaystyle\int_{\Delta S_j}\frac{\bar{I}_n^m(k,\mathbf{y},\mathbf{y}_c)}{\partial n(\mathbf{y})}\varphi_j\mathrm{d}S(\mathbf{y}), & \text{for } f_{ij}\varphi_j.\end{cases} \tag{15}$$

Information of a group of l source points $\mathbf{y}$ that are close to $\mathbf{y}_c$ can be added up and stored in one set of multipole moments $M_n^m(k,\mathbf{y}_c)$ given by:

$$M_n^m(k,\mathbf{y}_c) = \sum_l M_{n,l}^m(k,\mathbf{y}_c). \tag{16}$$

The multipole moment center can be moved from $\mathbf{y}_c$ to $\mathbf{y}_{c'}$ using the moment-to-moment (M2M) translation,

if $|\mathbf{y}-\mathbf{y}_{c'}| < |\mathbf{x}-\mathbf{y}_{c'}|$:

$$M_n^m(k,\mathbf{y}_{c'}) = \sum_{n'=0}^{\infty}\sum_{m'=-n'}^{n'}\sum_{\substack{l=|n-n'|\\ n+n'-l:\text{even}}}^{n+n'} \times(2n'+1)(-1)^{m'}W_{n,n',m,m',l}I_l^{-m-m'} \times(k,\mathbf{y}_c,\mathbf{y}_{c'})M_{n'}^{-m'}(k,\mathbf{y}_c), \tag{17}$$

where $W_{n,n',m,m',l}$ can be calculated using the following formula:

$$W_{n,n',m,m',l} = (2l+1)i^{n'-n+l}\begin{pmatrix} n & n' & l \\ 0 & 0 & 0\end{pmatrix} \times\begin{pmatrix} n & n' & l \\ m & m' & -m-m'\end{pmatrix}, \tag{18}$$

and $\begin{pmatrix} * & * & * \\ * & * & *\end{pmatrix}$ denotes the Wigner 3j symbol.

The multipole-to-local (M2L) translation, for the local expansion with the local expansion coefficients $L_n^m(k,\mathbf{x}_c)$, can be expressed as:

$$L_n^m(k,\mathbf{x}_c) = \sum_{n'=0}^{\infty}\sum_{m'=-n'}^{n'}\sum_{\substack{l=|n-n'|\\ n+n'-l:\text{even}}}^{n+n'} \times(2n'+1)(-1)^{m'}W_{n',n,m',m,l}\tilde{O}_l^{-m-m'} \times(k,\mathbf{x}_c,\mathbf{y}_c)M_{n'}^{m'}(k,\mathbf{y}_c), \tag{19}$$

where $|\mathbf{x}-\mathbf{x}_c| < |\mathbf{y}-\mathbf{x}_c|$ and $|\mathbf{y}-\mathbf{y}_c| < |\mathbf{x}-\mathbf{y}_c|$.

The local expansion center $\mathbf{x}_c$ can be moved to $\mathbf{x}_{c'}$ using local-to-local (L2L) translation, given $|\mathbf{x}-\mathbf{x}_{c'}| < |\mathbf{y}-\mathbf{x}_{c'}|$:

$$L_n^m(k,\mathrm{x}_{c'}) = \sum_{n'=0}^{\infty}\sum_{m'=-n'}^{n'}\sum_{\substack{l=|n-n'|\\ n+n'-l:\text{even}}}^{n+n'} \times(2n'+1)(-1)^{m}W_{n',n,m',-m,l}I_l^{m-m'} \times(k,\mathbf{x}_{c'},\mathbf{x}_c)L_{n'}^{m'}(k,\mathbf{x}_{c'}). \tag{20}$$

M2M, M2L, L2L translations are depicted in Fig. 1.

Finally, for a group of source points $\mathbf{y}_j$ that are far away from the collocation point $\mathbf{x}_i$, $g_{ij}q_j$ or $f_{ij}\varphi_j$ can be expressed in terms of the local expansion using the local expansion coefficients obtained from Eq. (19) or Eq. (20), which are functions of $\mathbf{x}_c$ and k only:

$$g_{ij}q_j \quad\text{or}\quad f_{ij}\varphi_j = \frac{ik}{4\pi}\sum_{n=0}^{\infty}(2n+1)\sum_{m=-n}^{n}L_n^m(k,x_c) \times\left[\bar{I}_n^m(k,x_i,x_c)+\alpha\frac{\partial\bar{I}_n^m(k,x_i,x_c)}{\partial n(x_i)}\right]. \tag{21}$$

For elements that are close to the collocation point $\mathbf{x}_i$, the conventional direct evaluation of the integrals (Eq. 9) will be used.

3 Adaptive FMM Algorithm

The adaptive FMM algorithm is described in the following subsections. It is a modified version of the one reported in [47] for 3-D potential problems.

The FMBEM uses the iterative solver GMRES in which the FMM is used to accelerate the vector λ and matrix $\mathbf{A}$ multiplication (Eq. 10). The adaptive FMM algorithm consists of the following three sects. 3.1–3.3:

3.1 Initialization

An adaptive hierarchical oct-tree of boxes is constructed by dividing the level 0 box enclosing the problem boundary into smaller and smaller boxes until the number of elements contained in each leaf (childless box) is less than the maximum number allowed in a box. On the same level, two boxes are said to be *colleagues* if they share at least a boundary point (a box is considered a colleague of itself), otherwise, they are said to be well separated. Every box b starting from level 2 has an *interaction list*, consisting of the children of colleagues of b's parent box, which are well separated from b.

3.2 Upward pass

Starting from the lowest level, the multipole moments are calculated for each box (Eqs. 15,16) and translated to the box's parent's center using M2M (Eq. 17). Continue the M2M translations until tree level 2 is reached. After the upward pass, every box down from level 2 should have a multipole moment set.

3.3 Downward pass

Starting from level 2 to the lowest level, the multipole moments of each box b at level l are translated, by using M2L translations (Eq. 19), to:

1. Boxes in the interaction list of b.
2. Level $l+1$ boxes that are separated from b (if b is a leaf) by a level $l+1$ box.
3. Level $l-1$ leafs that are separated from b by a level l box.

The local coefficients of box b are translated, using L2L translations (Eq. 20), to b's child boxes.

For box b at level l, calculate $g_{ij}q_j$ and $f_{ij}\varphi_j$ for each element i in b using Eq. (21). Add direct evaluation results (Eq. 9) for element i in box b and elements j in:

1. Boxes that are colleagues of b (if b is a leaf).
2. Leaves that are not b's colleages but share at least a boundary point with b (if b is a leaf).
3. Level l' ($l' > l+1$) boxes that are separated from b (if b is a leaf) by a level l' box.
4. Level l' ($l' < l-1$) leaves that are separated from b by a level l box.

After the downward pass, the vectors $g_{ij}q_j$ and $f_{ij}\varphi_j$ are calculated in the iterative solver.

3.4 Further improvements

Some improvements are made to further enhance the efficiency of the adaptive FMBEM.

3.4.1 Reuse of the preconditioner

The block diagonal preconditioner [50,51] used in the iterative solver (GMRES) stores some of the coefficients (g_{ij}, f_{ij} in Eq. (9)). In the implementation of the adaptive FMBEM, we calculate the preconditioner once and store it for all iterations. This provides an option to reuse these coefficients in the downward pass. Marked improvement can be achieved, especially when the numerical integration requires large numbers of quadrature points due to the strong variation of the kernels.

3.4.2 Storing coefficients

For problems with undesirable condition numbers, many iterations have to be carried out before the residue decreases below the tolerance. In each iteration, although the direct evaluation (Eq. 9) results are the same, the downward pass still performs direct evaluations in each iteration. In the adaptive FMBEM, we store all the coefficients calculated from Eq. (9) in the downward pass during the first iteration and use them for all the subsequent iterations. This leads to further savings in CPU time as can be seen in the numerical examples to be discussed next.

4 Numerical examples

The adaptive FMBEM has been implemented in a code using Fortran 90, and tested on several models of acoustic wave problems. Constant triangular elements are used in this study, for which one can use singularity subtraction approach for analytically evaluate the singular and hypersingular integrals involving the static kernels.

In all the examples, the maximum number of elements in a leaf is set to 100. The number of multipole and local expansion terms is set to 10. The GMRES solver will stop iterations when the residue is below the tolerance 10^{-3}. All the computations were done on a laptop PC with an Intel 1.6 GHz Centrino processor and 512 MB memory.

4.1 Radiation from a pulsating sphere

As the first example, a pulsating sphere with radius $a = 1$ m and normal velocity $v = 10$ m/s is used to verify the adaptive FMBEM for radiation problems. The normalized wave number ka varies from 1 to 10. The total number of elements is 1,200. The velocity potentials at $(5a, 0, 0)$ are plotted in Fig. 2, which shows that the conventional BEM with the CBIE fails to predict the surface velocity potential at the fictitious frequencies. The conventional BEM with the Burton–Miller (CHBIE) formulation compares well with the analytical solution at all wave numbers. The adaptive FMBEM with the CHBIE yields very close results to the conventional BEM with the CHBIE, which suggests that the truncation error introduced by fast multipole expansions is very small for problems with ka ranging from 1 to 10.

4.2 Scattering from a rigid sphere

As the second example, a rigid sphere with radius $a = 1$ m centered at $(0, 0, 0)$, is used to test the adaptive FMBEM for scattering problems. The sphere is meshed with 1,200 elements and impinged upon by an incident wave of unit amplitude $\varphi^I = \mathrm{e}^{-\mathrm{i}kz}$, with ka being one of the characteristic wave numbers, π, traveling along the negative z axis. Sample field points are evenly distributed on a circle of $r = 5a$, centered at $(0, 0, 0)$. The velocity potential curves plotted in Fig. 3 shows that the adaptive FMBEM using Burton–Miller formulation successfully overcomes the non-uniqueness difficulties at this fictitious frequency and yields very accurate results.

4.3 Convergence study and comparison of the computing efficiencies

In the first two examples, it has been shown that the adaptive FMBEM can successfully overcome the non-uniqueness difficulties in the BIE for exterior radiation and scattering problems. In this subsection, we analyze

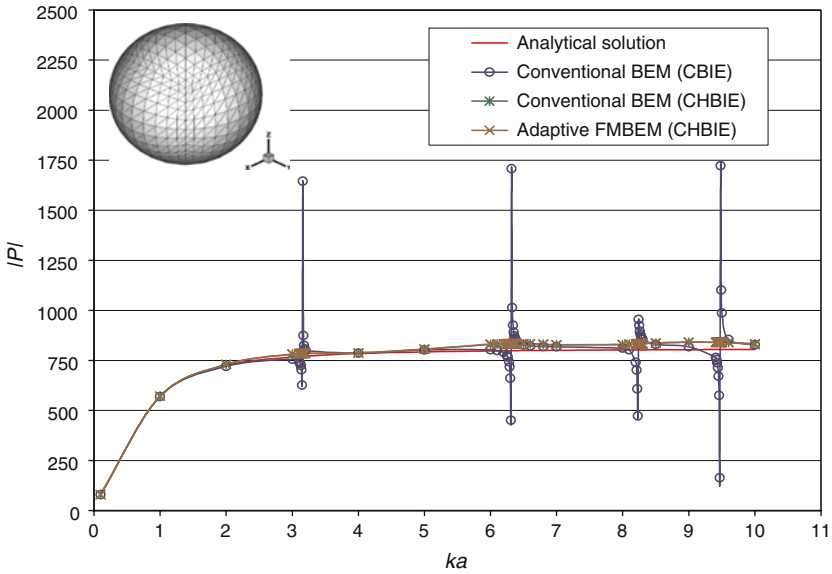

Fig. 2 Frequency sweep plot for the pulsating sphere model

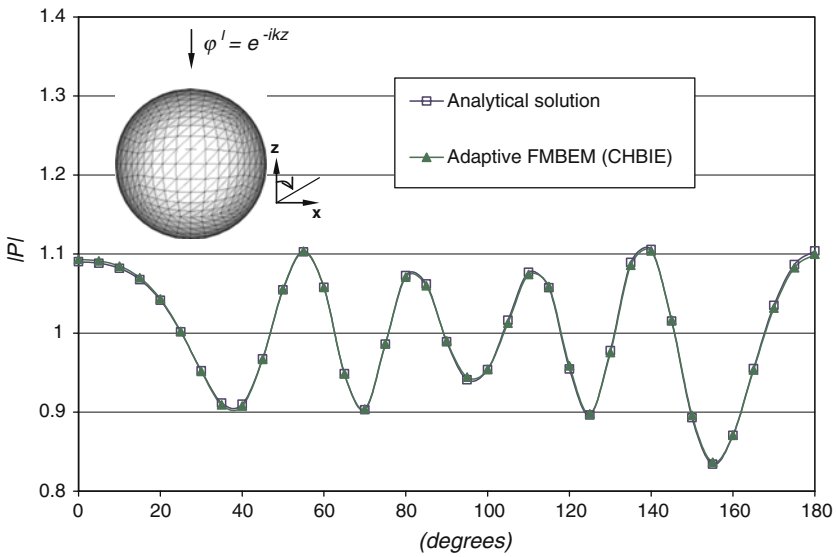

Fig. 3 Scattering from the rigid sphere at the fictitious frequency $ka = \pi$

the convergence behavior to further validate the adaptive FMBEM. Again, the pulsating sphere used in the first example is used here for which the exact solution is available. The *ka* is taken to be 1, and the number of expansion terms is 6. The sample point is taken at (5, 0, 0).

As shown in Fig. 4, the adaptive and non-adaptive FMBEM percentage-error curves are very close to that of the conventional BEM with the Burton–Miller formulation; and all errors decrease very fast as the number of elements increases, which further demonstrates the accuracy of the adaptive FMBEM.

The computational efficiencies of the adaptive FMBEM as compared with the non-adaptive FMBEM and the conventional BEM are shown in Fig. 5. It is seen from this figure that the adaptive FMBEM is faster than the conventional BEM for models with more than 1,000 elements. The adaptive FMBEM is also several times faster than the non-adaptive FMBEM. Due to the relatively small sizes of the models for the simple geometry, the computational efficiency of the adaptive FMBEM is not so obvious from Fig. 5. For larger models, to be shown in the last example, the order $O(N)$ computational efficiency of the adaptive FMBEM will be demonstrated.

4.4 An engine block model

We further explore the large-scale applicability of the adaptive FMBEM. The radiation of acoustic waves from

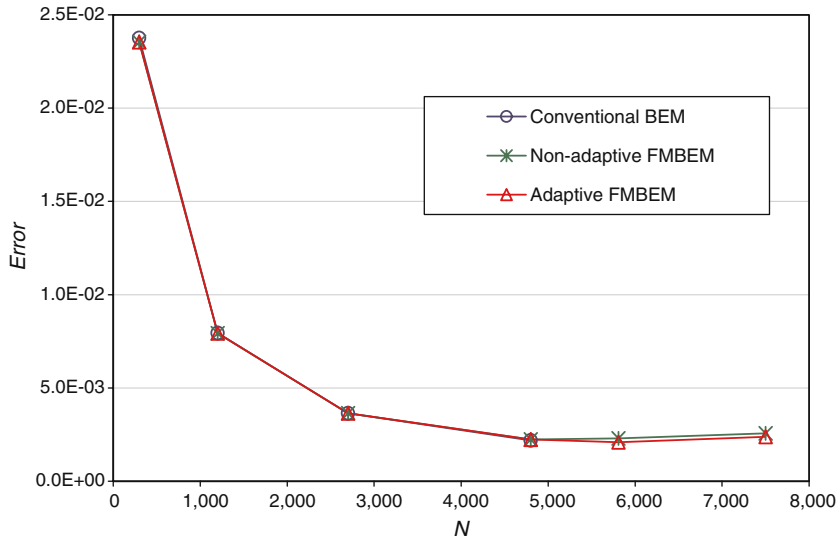

Fig. 4 Relative errors of the solutions for the pulsating sphere model

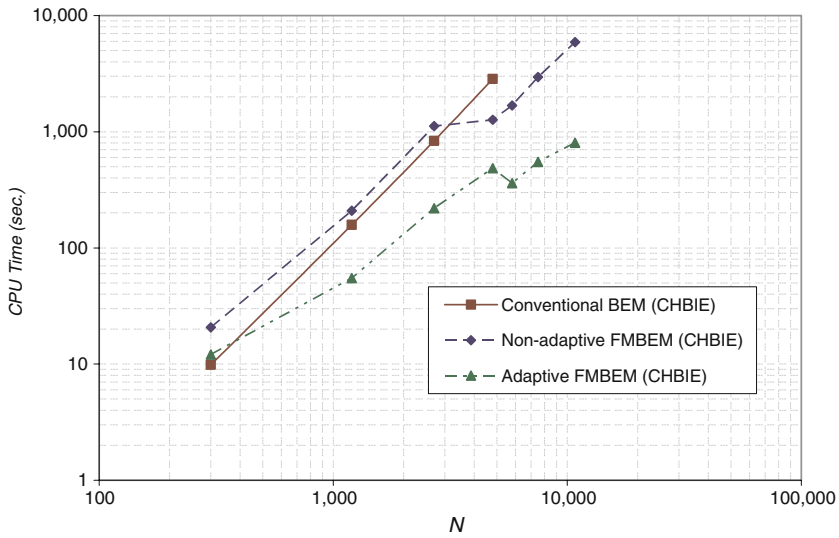

Fig. 5 Total CPU time used to solve the pulsating sphere model

an engine block is studied first. The engine block has a overall dimensions of 3.1 × 2.7 × 3.5 in the x, y and z direction, respectively, and is meshed with 37,482 constant triangular elements (Fig. 6). A monopole is placed inside each of the six cylinder holes to create the boundary conditions for the engine block. The wave number k of the monopole is 1. A total of 531 field points are placed on a semispherical data collection surface with radius of 10 to determine the velocity potential distribution. Figure 7 shows the computed velocity potential distribution on this data collection surface. The total CPU time used is 4,515 s for this model which has a relatively complicated geometry.

4.5 Scattering from multiple objects

A multi-scatterer model (Fig. 8) containing 1,000 randomly distributed capsule-like rigid scatterers in a 2 m × 2 m × 2 m domain is studied next. Each scatterer is meshed with 200 boundary elements (Fig. 8), with a total of 200,000 elements for the entire model. The incident wave is e^{-ikx} with $k = 1$. Sample points are taken at an annular data collection surface with inner and outer radius equal to 5 and 10, respectively. The computed velocity potential distribution contour is shown in Fig. 9 for this discretization. Total CPU time used to solve this large model is 3,352 s using the laptop PC. This mesh may not be fine enough to capture the interactions among the scatterers. However, this effect may be sufficiently small for the field away from the scatterers, such as that on the data collection surface used here. Models with refined meshes can be studied using a computer with a larger memory capacity.

To study the computational efficiency of the adaptive FMBEM for large-scale models, the BEM model is rerun with an increasing number of scatterers in the model.

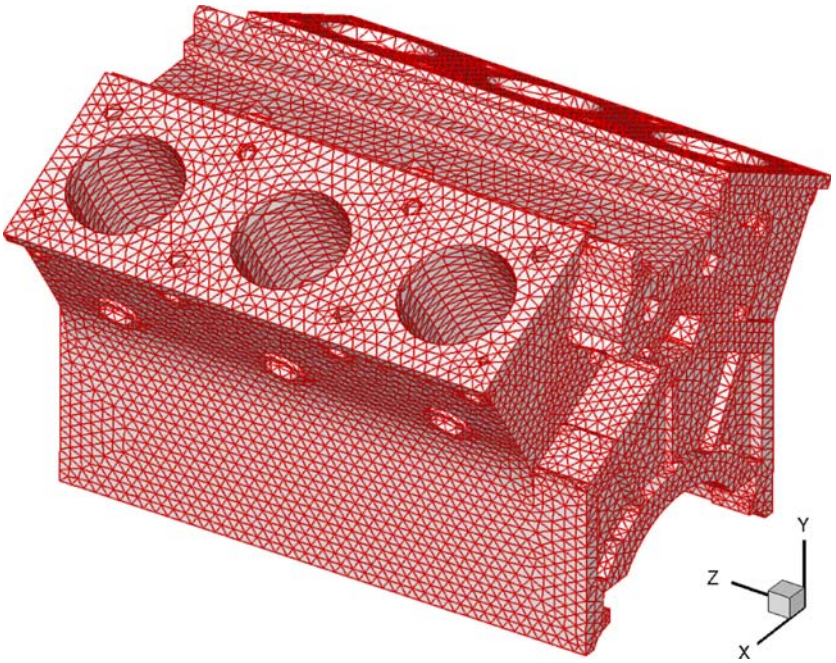

Fig. 6 An engine block model solved by the adaptive FMBEM

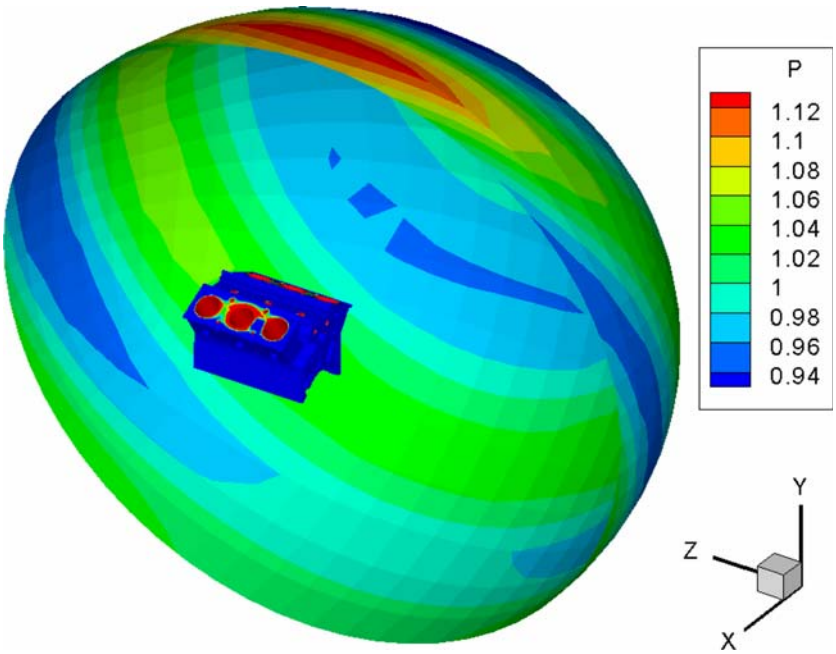

Fig. 7 Computed velocity potential for the engine block model

The numbers of elements are increased from 1,600 to 200,000, corresponding to 8 to 1,000 scatterers in the model. The total CPU time used to solve these multi-scatterer problems is shown in Fig. 10, which exhibits linear behavior and thus suggests the $O(N)$ efficiency of the developed adaptive FMBEM.

The above examples clearly demonstrate the potentials of the adaptive FMBEM based on the Burton–Miller BIE for solving large-scale acoustic wave problems. Further studies can be carried out to solve even larger scale industrial application problems using the developed code on high-end PCs, workstations or supercomputers.

5 Discussions

An adaptive fast multipole boundary element method is presented in this paper for solving 3-D acoustic wave problems. The Burton–Miller BIE formulation is

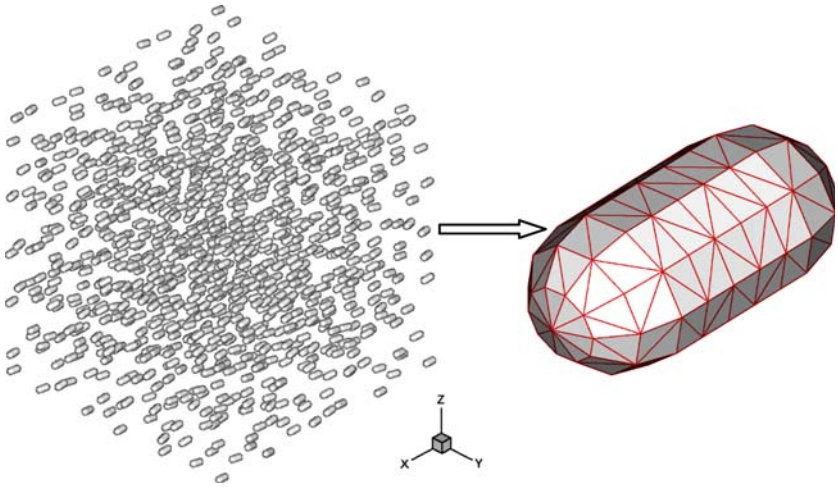

Fig. 8 A multi-scatterer model with 200,000 elements and the BEM mesh on each scatterer

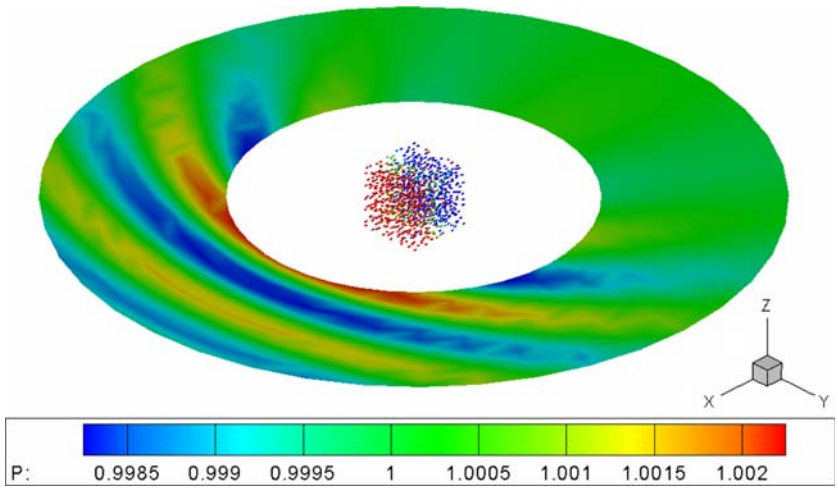

Fig. 9 Computed velocity potential for the multiple scatterer model

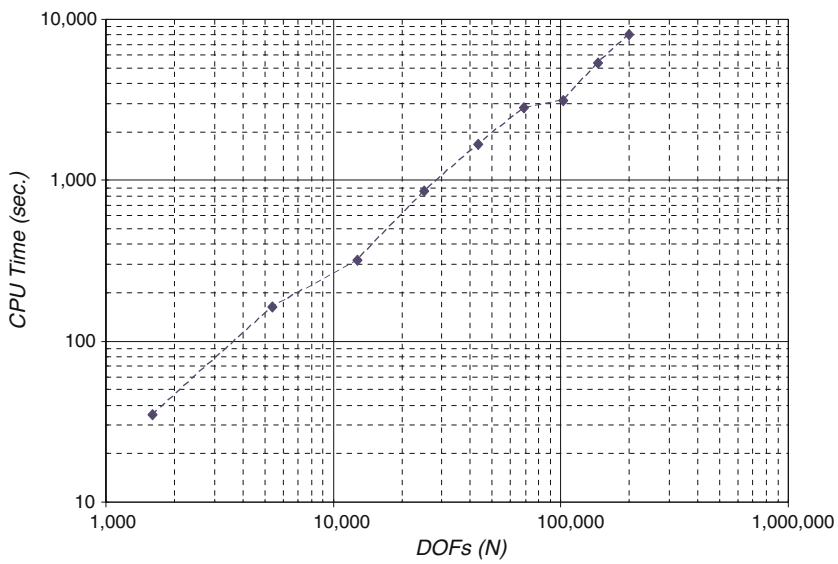

Fig. 10 Total CPU time used to solve the multi-scatterer problem

employed with the adaptive FMBEM so that the non-uniqueness difficulties associated with the conventional BIE for exterior domain problems are removed. It is found that the adaptive FMBEM can be several times faster than the non-adaptive FMBEM. Several radiation and scattering models including a model with 200,000 elements are solved successfully on a laptop PC. These examples clearly demonstrate that the adaptive FMBEM is ready to be used to solve large-scale practical problems.

More improvements can be made for the adaptive FMBEM. The FMM formulation for Helmholtz equation used in this study has the computational complexity of $O(p^5)$ for the M2M, M2L, L2L translations, where p is the expansion order. One may take the advantage of the recursive relations of the translation operators and use rotation-coaxial translation decomposition of the translation operators given by Gumerov and Duraiswami [36] to reduce the computational complexity to $O(p^3)$. The adaptive algorithm is also capable of accelerating this new FMM formulation. This will be the future work to improve the FMBEM.

The developed adaptive FMBEM can be extended to solve many other acoustic problems, for examples, half-space problems [52] and problems with thin structures. Furthermore, the adaptive fast multipole algorithm can be applied to solver other types of problems, such as 3-D elastostatic and elastodynamic problems.

Acknowledgments The work is supported in part by the grant CMS-0508232 of the US National Science Foundation. The authors would like to thank Mr. Jie Zhu for his help in creating the engine block CAD model used in this study. The authors would also like to thank the two reviewers for their constructive comments on the earlier version of this manuscript.

References

1. Brebbia CA, Dominguez, J (1989) Boundary elements — an introductory course. McGraw Hill, New York
2. Banerjee PK (1994) The boundary element methods in engineering. McGraw-Hill, New York
3. Copley LG (1967) Integral equation method for radiation from vibrating bodies. J Acoust Soc Am 41:807–810
4. Schenck HA (1968) Improved integral formulation for acoustic radiation problems. J Acoust Soc Am 44:41–58
5. Burton AJ, Miller GF (1971) The application of the integral equation methods to the numerical solution of some exterior boundary-value problems. In: Proceedings of the Royal Society of London, Series A, Math Phys Sci 323(1553):201–210
6. Meyer WL, Bell WA, Zinn BT (1978) Boundary integral solutions of three dimensional acoustic radiation problems. J Sound Vib 59(2):245–262
7. Terai T (1980) On calculation of sound fields around three dimensional objects by integral equation methods. J Sound Vib 69(1):71–100
8. Gentle JE (1998) Gaussian elimination. In Numerical linear algebra for applications in statistics. Springer, Berlin Heidelberg New York, pp 87–91
9. Saad Y, Schultz MH (1986) GMRES: a generalized minimal residual algorithm for solving nonsymmetric linear systems. SIAM J Sci Statist Comput 7:856–869
10. Sonneveld P (1989) CGS: a fast Lanczos-type solver for nonsymmetric linear systems. SIAM J Sci Statist Comput 10:36–52
11. Beylkin G, Coifman A, Rokhlin V (1991) Fast wavelet transforms and numerical algorithms I. Comm Pure Appl Math XLIV:141–183
12. Hackbusch W (1999) A sparse matrix arithmetic based on H-matrices I. Introduction to H-matrices. Computing 62(2):89–108
13. Golub G, Loan CV (1996) Matrix computations, 3rd edn. The Johns Hopkins University Press, Baltimore
14. Greengard L, Rokhlin V (1987) A fast algorithm for particle simulations. J Comput Phys 73:325–348
15. Rokhlin V (1988) A fast algorithm for the discrete Laplace transformation. J Complex 4(1):12–32
16. White CA, Head-Gordon M (1994) Derivation and efficient implementation of the fast multipole method. J Chem Phys 101(8):6593–6605
17. White CA, et al. (1994) The continues fast multipole method. Chem Phys Lett 230(1–2):8–16
18. White CA, Head-Gordon M (1996) Rotating around the quartic angular momentum barrier in fast multipole method calculations. J Chem Phys 105(12):5061–5067
19. Beatson R, Greengard L (1996) A short course on fast multipole methods. In: Ainsworth M, et al. (eds) Wavelets, multilevel methods and elliptic PDEs. Oxford University Press, pp 1–37
20. Cheng H, Greengard L, Rokhlin V (1999) A fast adaptive multipole algorithm in three dimensions. J Comput Phys 155(1):468–498
21. Rokhlin V (1990) Rapid solution of integral equations of scattering theory in two dimensions. J Comput Phys 86(2):414–439
22. Engheta N, et al. (1992) The fast multipole method (FMM) for electromagnetic scattering problems. IEEE Trans Ant Propag 40(6):634–641
23. Rokhlin V (1993) Diagonal forms of translation operators for the Helmholtz equation in three dimensions. Appl Comput Harmon Anal 1(1):82–93
24. Coifman R, Rokhlin V, Wandzura S (1993) The fast multipole method for the wave equation: a pedestrian prescription. IEEE Ant Propagat Mag 35(3):7–12
25. Lu C, Chew W (1993) Fast algorithm for solving hybrid integral equations. IEE Proceedings-H 140(6):455–460
26. Wagner R, Chew W (1994) A ray-propagation fast multipole algorithm. Microwave Opt Technol Lett 7:435–438
27. Epton M, Dembart B (1995) Multipole translation theory for the three dimensional Laplace and Helmholtz equations. SIAM J Sci Comput 16:865–897
28. Rahola J (1996) Diagonal forms of the translation operators in the fast multipole algorithm for scattering problems. BIT 36:333–358
29. Chen YH, Chew WC, Zeroug S (1997) Fast multipole method as an efficient solver for 2D elastic wave surface integral equations. Comput Mech 20(6):495–506
30. Song J, Lu C-C, Chew WC (1997) Multilevel fast multipole algorithm for electromagnetic scattering by large complex objects. IEEE Trans Ant Propag 45(10):1488–1493
31. Koc S, Chew WC (1998) Calculation of acoustical scattering from a cluster of scatterers. J Acoust Soc Am 103(2):721–734

32. Gyure MF, Stalzer MA (1998) A prescription for the multilevel Helmholtz FMM. IEEE Comput Sci Eng 5(3): 39–47
33. Greengard L, et al (1998) Accelerating fast multipole methods for the Helmholtz equation at low frequencies. IEEE Comput Sci Eng 5(3):32–38
34. Tournour MA, Atalla N (1999) Efficient evaluation of the acoustic radiation using multipole expansion. Int J Numer Methods Eng 46(6):825–837
35. Darve E (2000) The fast multipole method: Numerical implementation. J Comput Phys 160(1):195–240
36. Gumerov NA, Duraiswami R (2003) Recursions for the computation of multipole translation and rotation coefficients for the 3-D Helmholtz equation. SIAM J Sci Comput 25(4):1344–1381
37. Darve E, Havé P (2004) Efficient fast multipole method for low-frequency scattering. J Comput Phys 197(1):341–363
38. Fischer M, Gauger U, Gaul L (2004) A multipole Galerkin boundary element method for acoustics. Eng Anal Bound Elem 28(2):155–162
39. Chen JT, Chen KH (2004) Applications of the dual integral formulation in conjunction with fast multipole method in large-scale problems for 2D exterior acoustics. Eng Anal Bound Elem 28(6):685–709
40. Chew WC (1992) Recurrence relations for three-dimensional scalar and addition theorem. J Electromagn Waves Appl 6:133–142
41. Nishimura N (2002) Fast multipole accelerated boundary integral equation methods. Appl Mech Rev 55(4):299–324
42. Chen J, Hong H-K (1999) Review of dual boundary element methods with emphasis on hypersingular integrals and divergent series. Appl Mech Rev 52(1):17–33
43. Guiggiani M (1998) Formulation and numerical treatment of boundary integral equations with hypersingular kernels. In: Sladek V, Sladek J (eds) Singular integrals in boundary element methods. Computational Mechanics Publications, Boston
44. Krishnasamy GL, et al. (1990) Hypersingular boundary integral equations: some applications in acoustic and elastic wave scattering. J Appl Mech 57:404–414
45. Liu YJ, Rizzo FJ (1992) A weakly singular form of the hypersingular boundary integral equation applied to 3D acoustic wave problems. Comput Methods Appl Mech Eng 96: 271–287
46. Yang SA (2002) Evaluation of 2D Green's boundary formula and its normal derivative using Legendre polynomials, with an application to acoustic scattering problems. Int J Numer Methods Eng 53:905–927
47. Shen L, Liu YJ (2006) An adaptive fast multipole boundary element method for three-dimensional potential problems. Comput Mech (in press)
48. Kress R (1985) Minimizing the condition number of boundary integral operators in acoustic and electromagnetic scattering. Q J Mech Appl Math 38:323–341
49. Yoshida K-i (2001) Applications of fast multipole method to boundary integral equation method. Department of Global Environment Engineering, Kyoto University
50. Nishida T, Hayami K (1997) Application of the fast multipole method to the 3D BEM analysis of electron guns. In: Marchettia M, Brebbia CA, Aliabadi MH (eds) Boundary elements XIX. Computational Mechanics Publications, Boston, pp 613–622
51. Chen K, Harris PJ (2001) Efficient preconditioners for iterative solution of the boundary element equations for the three-dimensional Helmholtz equation. Appl Numer Math 36(4):475–489
52. Seybert AF, Wu TW (1989) Modified Helmholtz integral equation for bodies sitting on an infinite plane. J Acoust Soc Am 85(1):19–23